



Contents lists available at ScienceDirect

Physics Letters A

www.elsevier.com/locate/pla



# Pairing susceptibility of iron-based superconductors within a two-layer Hubbard model

Dan Wei<sup>a</sup>, Jingyao Wang<sup>a</sup>, Yang Wu<sup>a</sup>, Ying Liang<sup>a</sup>, Tianxing Ma<sup>a,b</sup>

<sup>a</sup> Department of Physics, Beijing Normal University, Beijing 100875, China

<sup>b</sup> Beijing Computational Science Research Center, Beijing 100193, China

## ARTICLE INFO

### Article history:

Received 18 July 2017

Received in revised form 16 October 2017

Accepted 25 October 2017

Available online xxxx

Communicated by L. Ghivelder

### Keywords:

Hubbard model

QMC

Pairing symmetry

## ABSTRACT

By using the determinant quantum Monte Carlo method, we studied the dominant pairing susceptibility of iron-based superconductors within an extended Hubbard model, which describes the underlying electronic structure of both iron pnictides and iron chalcogenides. The extended Hubbard model is constructed by two iron layers, each of which forms two sublattices on a square structure. Although the coupling between the two layers has different effects on the behavior of pairings in iron pnictides and iron chalcogenides, our non-biased numerical simulations reveal that the pairing with  $S_{xy}$  symmetry dominates over the studied parameter for both materials.

© 2017 Elsevier B.V. All rights reserved.

## 1. Introduction

The studies of iron-based superconductors were motivated [1–4] by the discovery of superconductivity in fluorine-doped LaFeAsO by Hideo Hosono and co-workers in 2008 [1]. Since then, many experimental and theoretical efforts have been made to gain a better understanding of the mechanism of high temperature superconductivity; such efforts have been at the heart of modern condensed matter physics for more than 30 years after the observation of 40K superconductivity was first reported in doped cuprates [5]. Despite these extensive experimental research studies, the mechanism of superconductivity in these materials is controversial. The traditional theory of superconductivity, which is based on electron–phonon interactions, does not adequately describe the high temperature superconductivity phenomenon [6], and it has been suggested that strong electronic correlation may drive such unconventional superconductivity, which may be governed by the two-dimensional (2D) Hubbard model (or, the large  $U$  limit,  $t$ - $J$  model) on various lattice structures [7,9,8]. The 2D Hubbard model is a basic electronic model in solid state physics, and obtaining a non-perturbative solution of the 2D Hubbard model is a difficult task in current condensed matter physics [10].

Iron-based high-temperature superconductors are layered materials with complicated electronic structures. According to their electronic structures, the iron-based superconductors can be clas-

sified into two large families: the first family consists of iron pnictides and Fe(Te, Se) bulk crystals [11–13], and the second family consists of  $A_x\text{Fe}_{2-y}\text{Se}_2$  ( $A = \text{K, Rb, Cs, Tl/K}$ ) [14–17]. Unlike conventional superconductors, for which the Cooper pairing mechanism is well established [6], the complexity of iron-based superconductor electronic structures leads to major difficulties in understanding pairing symmetry [18,19].

It is possible to obtain some unbiased results for the one- or two-band (or orbit) Hubbard model on a fairly large lattice by using quantum Monte Carlo methods [20]; for the microscopic electronic structure that leads to superconductivity in iron-based superconductors, various models containing different numbers of  $d$ -orbitals, whose numbers range from two to five, have been proposed [21–26]. Although they might offer a better perspective on the mechanism of iron-based superconductors, analysis of more orbitals results in the introduction of more parameters and thus makes calculations more difficult [19,27–36]. Recently, a two-orbital model with  $S_4$  symmetry has been proposed [26]. The model includes two nearly degenerate and weakly coupled single-orbital parts that can be mapped to each other under the  $S_4$  transformation. Further, the two-orbit model can essentially be decoupled into two nearly degenerate one-orbit models, and the two  $d$ -orbitals are divided in two groups, as shown in Fig. 1; one group, for example, the up layer, includes the  $d_{x'z}$  orbital in the  $A$  sublattice, and the  $d_{y'z}$  orbital in the  $B$  sublattice, and the other includes the  $d_{x'z}$  orbital in the  $B$  sublattice and the  $d_{y'z}$  orbital in the  $A$  sublattice, where  $A$  and  $B$  label the two sublattices of the iron square lattices, following Ref. [26], and the square lattice structure

E-mail address: liang@bnu.edu.cn (Y. Liang).

<https://doi.org/10.1016/j.physleta.2017.10.049>

0375-9601/© 2017 Elsevier B.V. All rights reserved.

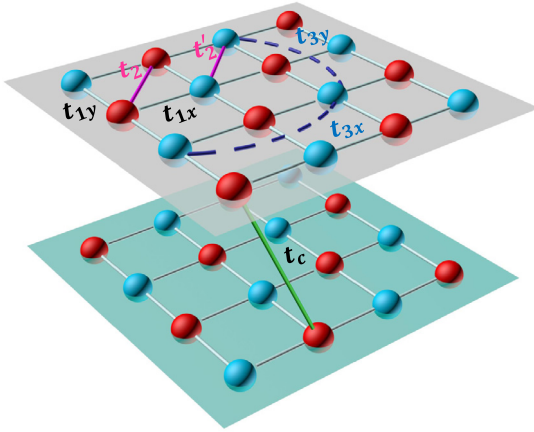


**Fig. 1.** (Color online.) The sketch shown here is based on Ref. [26], where the structures of the  $d_{xz}$  and  $d_{yz}$  orbitals are shown. The hopping parameters are indicated as follows: the nearest-neighbor hopping parameters are  $t_{1x}$  and  $t_{1y}$ , the next-nearest-neighbor hopping parameters are  $t_2$  and  $t'_2$ , and the third next-nearest-neighbor hopping parameters are  $t_{3x}$  and  $t_{3y}$ . The coupling between the two groups is denoted by the nearest-neighbor hopping  $t_c$ .

of a single iron layer shows two Fe iron atoms shown in different colors that form two sublattices. As shown in the figures, the hopping parameters  $t_{1x}$  and  $t_{1y}$  indicate the nearest-neighbor hopping,  $t_2$  and  $t'_2$  indicate the next-nearest-neighbor hopping (which break symmetry along two different diagonal directions),  $t_{3x}$  and  $t_{3y}$  indicate the third nearest-neighbor hopping, and  $t_c$  indicates by the nearest-neighbor hopping corresponding to the coupling between two layers.

Without turning on the couplings between the two layers, some of the authors of this study have performed a quantum Monte Carlo study of the pairing correlation in the  $S_4$  symmetric microscopic model [37,38]. It was found that the pairing with an extensive  $s$ -wave symmetry robustly dominates over other pairings at low temperature in a reasonable parameter region, regardless of the change in Fermi surface topologies; this result provides a possible unified understanding of the superconducting mechanism in iron-pnictides and iron-chalcogenides. Similarly to doped cuprates [39,40], the interlayer coupling may also be key to understanding the superconducting mechanism. For example, the nature of the  $c$ -axis charge dynamics in doped cuprates is of great importance because the mechanism of superconductivity is closely related to the anisotropic normal-state properties. The introduction of interlayer hopping  $t_c$  may also result in the change in the Fermi surface as well as the band dispersions of iron-based superconductors [26]. Thus, it is necessary to examine the effect of the interlayer coupling on the behavior of pairing susceptibility.

By using the determinant quantum Monte Carlo method, we studied the dominant pairing susceptibility of iron-based superconductors on a double layer lattice for both iron pnictides and iron chalcogenides, and our simulation was performed on a  $2 \times 8^2$  lattice, where '2' means two layers, and for each layer, the sites number is  $8^2$ , which is fairly large enough for the square lattice. Although the coupling between the two layers has different effects on the behavior of pairings in iron pnictides and iron chalcogenides, our non-biased numerical simulations reveal that the pairing with  $S_{xy}$  symmetry dominates over the studied parameter for both of materials.

## 2. Model and method

The Hamiltonian for each layer can be described as

$$\begin{aligned}
 H_m = & \sum_{i\sigma} [(t_{1x} a_{mi\sigma}^\dagger b_{mi\pm\hat{x}\sigma} + t_{1y} a_{mi\sigma}^\dagger b_{mi\pm\hat{y}\sigma}) + h.c] \\
 & + t_2 [\sum_{i\sigma} a_{mi\sigma}^\dagger a_{mi\pm(\hat{x}+\hat{y})\sigma} + \sum_{i\sigma} b_{mi\sigma}^\dagger b_{mi\pm(\hat{x}-\hat{y})\sigma}] \\
 & + t'_2 [\sum_{i\sigma} a_{mi\sigma}^\dagger a_{mi\pm(\hat{x}-\hat{y})\sigma} + \sum_{i\sigma} b_{mi\sigma}^\dagger b_{mi\pm(\hat{x}+\hat{y})\sigma}] \\
 & + \sum_{i\sigma} [(t_{3x} a_{mi\sigma}^\dagger b_{mi\pm 2\hat{x}\sigma} + t_{3y} a_{mi\sigma}^\dagger b_{mi\pm 2\hat{y}\sigma}) + h.c] \\
 & + U \sum_{mi} (n_{mai\uparrow} n_{mai\downarrow} + n_{mbi\uparrow} n_{mbi\downarrow}) \\
 & + \mu \sum_{mi\sigma} (n_{mai\sigma} + n_{mbi\sigma})
 \end{aligned} \tag{1}$$

where  $m = 1, 2$  indicating different layers, and the coupling between the two layers is given by

$$H_c = \sum_{i\sigma} 2t_c (a_{1i\sigma}^\dagger b_{2i\sigma} + h.c)$$

Here,  $a_{mi\sigma}$  ( $a_{mi\sigma}^\dagger$ ) annihilates (creates) electrons at the site  $R_{mi}$  with spin  $\sigma$  ( $\sigma = \uparrow, \downarrow$ ) on sublattice A of  $m$  group,  $b_{mi\sigma}$  ( $b_{mi\sigma}^\dagger$ ) annihilates (creates) electrons at the site  $R_{mi}$  with spin  $\sigma$  ( $\sigma = \uparrow, \downarrow$ ) on sublattice B of  $m$  group,  $n_{mai\sigma} = a_{mi\sigma}^\dagger a_{mi\sigma}$ ,  $n_{mbi\sigma} = b_{mi\sigma}^\dagger b_{mi\sigma}$ .  $U$  denotes the on-site Hubbard interaction. In the above model, for simplicity and clarity, we retain only a minimum set of parameters, including the three key shortest hopping parameters responsible for the physical picture revealed by the  $S_4$  symmetry.

To study the superconducting property, we computed its pairing susceptibility

$$P_\alpha = \frac{1}{N_s} \sum_{m,i,j} \int_0^\beta d\tau \langle \Delta_{m\alpha}^\dagger(i, \tau) \Delta_{m\alpha}(j, 0) \rangle \tag{2}$$

Where  $\alpha$  denotes the pairing symmetries  $S_{xy}$ ,  $d_{xy}$ ,  $S_{x^2-y^2}$ ,  $d_{x^2-y^2}$ , and  $\Delta_{m\alpha}^\dagger(i)$  is defined as

$$\Delta_{m\alpha}^\dagger(i) = \sum_l f_\alpha^\dagger(\delta_l) (a_{mi\uparrow} b_{mi+\delta_l\downarrow} - a_{mi\downarrow} b_{mi+\delta_l\uparrow})^\dagger$$

Here, the vectors  $\delta_l$  ( $l = 1, 2, 3, 4$ ) denote the nearest neighbor inter-sublattice connections, where  $\delta$  is  $(\pm\hat{x}, 0)$  and  $(0, \pm\hat{y})$ , or the next nearest neighbor inner-sublattice connections, where  $\delta'$  is  $(\pm(\hat{x}, \hat{y}))$  and  $(\pm(\hat{x}, -\hat{y}))$ . We studied four types of pairing forms. For  $S_{x^2+y^2}$ -wave pairing,  $f_{S_{x^2+y^2}}(\delta_l) = 1$ . For  $d_{x^2-y^2}$  pairing,  $f_{d_{x^2-y^2}}(\delta_l)$  is 1 when  $\delta_l = (\pm\hat{x}, 0)$  and  $-1$  otherwise. For the  $S_{xy}$ -wave and the  $d_{xy}$ -wave:

$$f_{d_{xy}}(\delta'_l) = 1 (\delta'_l = \pm(\hat{x}, \hat{y}))$$

$$f_{d_{xy}}(\delta'_l) = -1 (\delta'_l = \pm(\hat{x}, -\hat{y}))$$

$S_{xy}$ -wave:

$$f_{S_{xy}}(\delta'_l) = 1, l = 1, 2, 3, 4$$

## 3. Results and discussion

We first studied the pairing susceptibility and the effective pairing interaction for which  $t_c = 0.3$ , as shown in Fig. 2. Here, we defined  $t_{2s} = (t_2 + t'_2)/2$ , and as  $t_{2s} = 0.2$ , it describes iron chalcogenides without hole pockets. For simplify, we take  $t_1 = t_{1x} = t_{1y} = 0.3$ , and  $t_{3x} = t_{3y} = 0$ . It can be seen that, for either  $\langle n \rangle = 1.0$  or  $\langle n \rangle = 0.9$ , the pairing susceptibility increases as the temperature is

Download English Version:

<https://daneshyari.com/en/article/8204389>

Download Persian Version:

<https://daneshyari.com/article/8204389>

[Daneshyari.com](https://daneshyari.com)